Published in final edited form as:
Science. 2014 July 4; 345(6192): 98–101. doi:10.1126/science.1254312.

Opposing unfolded-protein-response signals converge on death receptor 5 to control apoptosis

Min Lu[1,*], **David A. Lawrence**[1,*], **Scot Marsters**[1], **Diego Acosta-Alvear**[2,3], **Philipp Kimmig**[2,3], **Aaron S. Mendez**[2,3], **Adrienne W. Paton**[4], **James C. Paton**[4], **Peter Walter**[2,3], and **Avi Ashkenazi**[1]

[1]Cancer Immunology, Genentech, Inc. 1 DNA Way South San Francisco, CA 94080, USA

[2]Howard Hughes Medical Institute, University of California at San Francisco, San Francisco, CA 94158, USA

[3]Department of Biochemistry and Biophysics, University of California at San Francisco, San Francisco, CA 94158, USA

[4]Research Centre for Infectious Diseases, School of Molecular and Biomedical Science, University of Adelaide, South Australia, 5005, AU

Abstract

Protein folding by the endoplasmic reticulum (ER) is physiologically critical, while its disruption causes ER stress and augments disease. ER stress activates the unfolded protein response (UPR) to restore homeostasis. If stress persists, the UPR induces apoptotic cell death, but the mechanisms remain elusive. Here we find that unmitigated ER stress promotes apoptosis through cell-autonomous, UPR-controlled activation of death receptor 5 (DR5). ER stressors induced *DR5* transcription via the UPR mediator CHOP; however, the UPR sensor IRE1α transiently catalyzed *DR5* mRNA decay, allowing time for adaptation. Persistent ER stress built up intracellular DR5 protein, driving ligand-independent DR5 activation and apoptosis engagement via caspase-8. Thus, DR5 integrates opposing UPR signals to couple ER stress and apoptotic cell fate.

The endoplasmic reticulum (ER) mediates folding and maturation of transmembrane and secreted proteins (1, 2). Elevated physiological demand for protein folding can cause misfolded proteins to accumulate in the ER lumen – a condition called ER stress. The UPR senses such stress and mediates cellular adaptation by expanding the ER's protein-folding capacity while decreasing its synthetic load. Protein kinase R (PKR)-like kinase (PERK) and inositol-requiring enzyme 1α (IRE1α) are two key metazoan UPR sensors (1, 2): residing in the ER membrane, each has a luminal domain that detects misfolded polypeptides. PERK harbors a cytoplasmic kinase moiety that phosphorylates eukaryotic translation-initiation factor α (eIF2α). This suppresses general translation but promotes synthesis of preferred factors including ATF4, which activates the UPR transcription factor C/EBP homologous protein (CHOP) amongst other genes. IRE1α has both kinase and endoribonuclease (RNase)

Correspondence to: Peter Walter; Avi Ashkenazi.
*Authors contributed equally to this work.

cytoplasmic moieties (3). The kinase controls RNase activity, which mediates regulated IRE1α-dependent decay (RIDD) of ER-associated mRNAs (4), and generates the UPR transcription factor X-box binding protein 1 spliced (XBP1s). Certain pathological conditions can cause irresolvable ER stress (5), often leading to apoptotic cell death (1, 2, 6). Two interconnected signaling cascades control apoptosis: the intrinsic, mitochondrial pathway, and the extrinsic, death-receptor pathway (7). Each engages distinct proteases, called initiator caspases, to activate a common set of executioner caspases (8). Unmitigated ER stress regulates the intrinsic pathway via several Bcl-2-family proteins (1, 2, 6, 9, 10). Furthermore, IRE1α cleaves specific micro-RNAs to de-repress caspase-2 expression (11); however, caspase-2 may be dispensable for ER stress-induced apoptosis (12), leaving the underlying initiation mechanisms obscure.

Experiments with biological and pharmacological ER stressors revealed consistent activation of caspase-8 — the pivotal initiator in the extrinsic pathway (8) (Fig. 1). The bacterial AB5 subtilase cytotoxin SubAB induces pathophysiological ER stress by cleaving the chaperone Bip (13). SubAB caused dose-dependent Bip depletion and ER stress, evident by CHOP and XBP1s upregulation, in KMS11 multiple myeloma cells (Fig. 1A). In keeping with data that PERK activity persists while IRE1α activation is transient (14), CHOP remained elevated whereas XBP1s declined by 24 hr. SubAB also induced activation of caspase-8 and caspase-3 by 24 hr, evident by cleaved caspase and poly-ADP ribose polymerase (PARP) products. SubAB substantially increased caspase-8 and caspase-3/7 enzymatic activity, and DNA fragmentation — an apoptotic hallmark (fig. S1 A to C). Brefeldin-A (BfA) — an inhibitor of ER-to-Golgi trafficking — similarly induced ER stress, caspase activation and apoptosis in SK-MES-1 lung carcinoma cells (Fig. 1B, and fig. S1 D to F). The sarcoplasmic ER calcium-ATPase inhibitor thapsigargin (Tg) induced persistent CHOP and transient XBP1s expression in wildtype and in *Bax*$^{-/-}$ HCT116 colon carcinoma cells; whereas apoptosis required *Bax*, caspase-8 activation did not (Fig. 1 C and D, and fig. S1 G to I). Moreover, siRNA depletion of caspase-8, but not caspase-2, blocked activation of caspase-3/7 and apoptosis by diverse ER stressors (Fig. 1 E and F, and fig. S1 J to O). Caspase-8 activates the Bcl-2-family protein Bid to engage the intrinsic pathway via Bax (15, 16). Full-length Bid declined in association with Tg-induced caspase-8 activation (fig. S1I), indicating Bid processing. Bid siRNA knockdown commensurately attenuated Tg-induced apoptosis, while caspase-8 siRNA inhibited both Bid processing and apoptosis (fig. S1 P to S). Tg also upregulated Bim (fig. S1I) as reported (10); however, caspase-8 and Bid processing occurred much earlier, suggesting that Bim might support later apoptotic signals. Thus, caspase-8 plays a pivotal role, whereas caspase-2 appears dispensable, during apoptosis induction by unmitigated ER stress.

Upon binding of cognate extracellular ligands, the death receptors Fas, DR4 or DR5 nucleate a death-inducing signaling complex (DISC) at the plasma membrane, activating caspase-8 via the adaptor Fas-associated death domain (FADD) (17). Consistent with evidence that ER stress upregulates *DR5* transcription (18), quantitative RT-PCR (QPCR) showed a 2–4 fold *DR5* mRNA induction by Tg, BfA, SubAB, or the glycosylation inhibitor tunicamycin (Tm), with less impact on *DR4*, *Fas*, or *TNFR1* (Fig. 2 A and B, and fig. S2 A to C). ER stressors most often elevated both the long (DR5L) and short (DR5S) splice

variants of DR5 (Fig. 2C and fig. S2 D to H) (19). Tg upregulated DR5 within 6 hr, in concert with CHOP and XBP1s induction, yet preceding caspase-8 processing (Fig. 2C and fig. S2D). Furthermore, Tg induced a DR5-nucleated complex with FADD and caspase-8, harboring elevated caspase-8 activity, independent of *Bax* (Fig. 2D and fig. S2 I to K). Immunoprecipitation (IP) of DR5 or caspase-8 showed comparable caspase-8 activity (fig. S2L). Consistently, other ER stressors increased DR5-associated caspase-8 activity in multiple cell lines (fig. S2 M to O). Livers from Tm-treated mice also showed elevated DR5 and cleaved caspase-8 in conjunction with apoptosis (fig. S2 P and Q). DR5 siRNA knockdown in different cell lines strongly inhibited caspase activation and apoptosis in response to various ER stressors (Fig. 2 E to H, and fig. S2 R to X). Thus, DR5 is critical for caspase-8-mediated apoptotic engagement by unmitigated ER stress.

Remarkably, siRNA depletion of the sole DR5 ligand, Apo2L/TRAIL, had no impact on Tg-induced apoptosis in HCT116 or SK-MES-1 cells, unlike caspase-8 knockdown (Fig. 3A and fig. S3 A and B). Moreover, neutralization of extracellular Apo2L/TRAIL using soluble DR4- and DR5-Fc fusion proteins, which blocked exogenously added ligand, did not inhibit apoptosis activation by Tg or BfA (Fig. 3B and fig. S3 C and D). Thus, ER stress induces ligand-independent DR5 activation. DR5 was barely detectable by immunofluorescence in resting SK-MES-1 cells, but showed higher abundance upon Tm, Tg, or BfA addition (Fig. 3C). In Tg-treated cells, DR5 co-localized with the Golgi marker RACS1, but not the ER marker KDEL; however, in BfA-treated cells — which had minimal Golgi — DR5 did co-localize with KDEL (Fig. 3D and fig. S3 E and F). Despite massively elevating total DR5, BfA did not substantially upregulate cell-surface DR5, nor did it increase sensitivity to exogenous Apo2L/TRAIL (fig. S3 G to J). However, Tg, which upregulated both total and cell-surface DR5, did enhance sensitivity to added ligand (fig. S3 K to N). DR5 partially co-localized with cleaved caspase-8 within Tg-treated cells (fig. S3O), supporting intracellular activation. Size-exclusion chromatography of detergent extracts from HCT116 cells revealed Tg-driven upregulation of DR5L and DR5S in low molecular weight (MW) fractions — representing DR5 oligomers; elevated DR5L appeared also in high MW fractions — indicating DR5L multimers (Fig. 3E). Caspase-8 activity occurred in two peaks: one coinciding with DR5L in high MW fraction, the other separate from DR5 in low MW compartments (Fig. 3F). Chemical crosslinking verified Tg-induced formation of DR5 oligomers and multimers (fig. S3P). Furthermore, selective DR5L siRNA knockdown attenuated Tg-driven activation of caspase-8 and apoptosis (fig. S3 Q to T). Thus, Tg upregulates both DR5 variants but DR5L preferentially multimerizes, recruiting and activating caspase-8 and releasing processed enzyme into lower MW fractions.

Consistent with earlier evidence (18, 20), siRNA depletion of CHOP substantially blocked *DR5* mRNA upregulation by Tg or BfA, whereas knockdown of the CHOP transcriptional targets ER oxidase 1α (ERO) 1α or growth arrest and DNA damage inducible 34 (GADD34) did not (Fig. 4A and fig. S4 A to E), supporting direct CHOP control of *DR5* mRNA. While GADD34 dephosphorylates eIF2α to re-initiate translation, ERO1α is important for protein disulfide isomerization and folding in the ER lumen (6). ERO1α knockdown did inhibit DR5L protein upregulation and the associated apoptotic events (fig. S4 F to H), suggesting that ERO1α may facilitate folding of DR5L (which harbors more

cysteine residues than DR5S). In contrast to CHOP depletion, siRNA knockdown of IRE1α attenuated *DR5* mRNA decay in Tg-treated cells (Fig. 4B and fig. S4 I to L), suggesting that IRE1α counteracts apoptosis by mediating *DR5* RIDD. Indeed, a recombinant protein comprising IRE1α's catalytic domains cleaved in vitro-transcribed *DR5* mRNAs at discrete sites, and this was blocked by the IRE1α RNase inhibitor 4μ8c (21) (Fig. 4C and fig. S4M). Furthermore, whereas CHOP siRNA attenuated Tg-induced DR5 upregulation, caspase-8 activation, and apoptosis, IRE1α depletion augmented these events (Fig. 4D and E, and fig. S4N). Conversely, XBP1s knockdown — which led to compensatory IRE1α hyperphosphorylation (Fig. 4D) as reported (22) — accelerated *DR5* mRNA decay and diminished DR5 upregulation, caspase-8 activation and apoptosis (Fig. 4 B, D and E, and fig. S4 I to L and N). Finally, 4μ8c enhanced caspase activation by Tg (Fig. 4F and fig. S4O), confirming an anti-apoptotic role for IRE1α RNase. Thus, CHOP and RIDD exert opposing effects on *DR5* to control caspase-8 activation and apoptosis.

Our data delineates a cell-autonomous mechanism wherein DR5 integrates dynamic UPR signals to control apoptosis in relation to ER stress (Fig. S4P). Upon reversible ER disruption, PERK-CHOP activity induces whereas RIDD suppresses, *DR5* transcripts. If ER stress resolves, UPR activity subsides and *DR5* mRNA returns to baseline. However, if ER stress prevails, PERK-CHOP function persists, while IRE1α activity attenuates (14), permitting *DR5* mRNA to rise. DR5 accumulation in the ER and Golgi apparatus drives ligand-independent multimerization of DR5L, which — consistent with earlier data (23) — has greater propensity to cluster than DR5S. ERO1α, previously implicated in UPR-driven apoptosis (6), facilitates DR5L upregulation, perhaps by supporting disulfide isomerization. DR5L provides a DISC-like intracellular platform for caspase-8 recruitment and apoptosis initiation. It was proposed that ER stress augments apoptosis by increasing autocrine death-ligand signaling (18, 24, 25); however, ER disruption would attenuate ligand secretion. Our data reveal that *DR5* acts as an intracellular "gauge" for persistence of ER stress. Opposing controls on *DR5* mRNA synthesis and decay by PERK-CHOP versus IRE1α define a time window for adaptation, before committing the cell to an apoptotic fate.

Supplementary Material

Refer to Web version on PubMed Central for supplementary material.

Acknowledgements

We thank Robert Pitti and Genentech's peptide, DNA and chemical synthesis and FACS labs for assistance.

References and notes

1. Walter P, Ron D. Science. 2011; 334:1081–1086. [PubMed: 22116877]
2. Hetz C. Nat. Rev. Mol. Cell Biol. 2012; 13:89–102. [PubMed: 22251901]
3. Korennykh A, Walter P. Annu Rev Cell Dev Biol. 2012; 28:251–277. [PubMed: 23057742]
4. Hollien J, Weissman JS. Science. 2006; 313:104–107. [PubMed: 16825573]
5. Wang S, Kaufman RJ. J. Cell Biol. 2012; 197:857–867. [PubMed: 22733998]
6. Tabas I, Ron D. Nat. Cell Biol. 2011; 13:184–190. [PubMed: 21364565]
7. Danial NN, Korsmeyer SJ. Cell. 2004; 116:205–219. [PubMed: 14744432]

8. Salvesen GS, Ashkenazi A. Cell. 2011; 147:476–476. [PubMed: 22000022]
9. Zinszner H, et al. Genes Dev. 1998; 12:982–995. [PubMed: 9531536]
10. Puthalakath H, et al. Cell. 2007; 129:1337–1349. [PubMed: 17604722]
11. Upton J-P, et al. Science. 2012; 338:818–822. [PubMed: 23042294]
12. Sandow JJ, et al. Cell Death Differ. 2014; 21:475. [PubMed: 24292555]
13. Paton AW, et al. Nature. 2006; 443:548–552. [PubMed: 17024087]
14. Lin JH, et al. Science. 2007; 318:944–949. [PubMed: 17991856]
15. Li HL, et al. Cell. 1998; 94:491–501. [PubMed: 9727492]
16. LeBlanc H, et al. Nat. Med. 2002; 8:274–281. [PubMed: 11875499]
17. Wilson NS, Dixit V, Ashkenazi A. Nat. Immunol. 2009; 10:348–355. [PubMed: 19295631]
18. Yamaguchi H, Wang HG. J. Biol. Chem. 2004; 279:45495–45502. [PubMed: 15322075]
19. Sheridan JP, et al. Science. 1997; 277:818–821. [PubMed: 9242611]
20. Abdelrahim M, et al. Carcinogenesis. 2006; 27:717–728. [PubMed: 16332727]
21. Cross BCS, et al. Proc. Natl. Acad. Sci. U.S.A. 2012; 109:869–878. [PubMed: 22219365]
22. Niederreiter L, et al. J. Exp. Med. 2013; 210:2041–2056. [PubMed: 24043762]
23. Wagner KW, et al. Nat. Med. 2007; 13:1070–1077. [PubMed: 17767167]
24. Martin-Perez R, Niwa M, Lopez-Rivas A. Apoptosis. 2012; 17:349–363. [PubMed: 22072062]
25. Hu P, Han Z, Couvillon AD, Kaufman RJ, Exton JH. Mol. Cell. Biol. 2006; 26:3071–3084. [PubMed: 16581782]

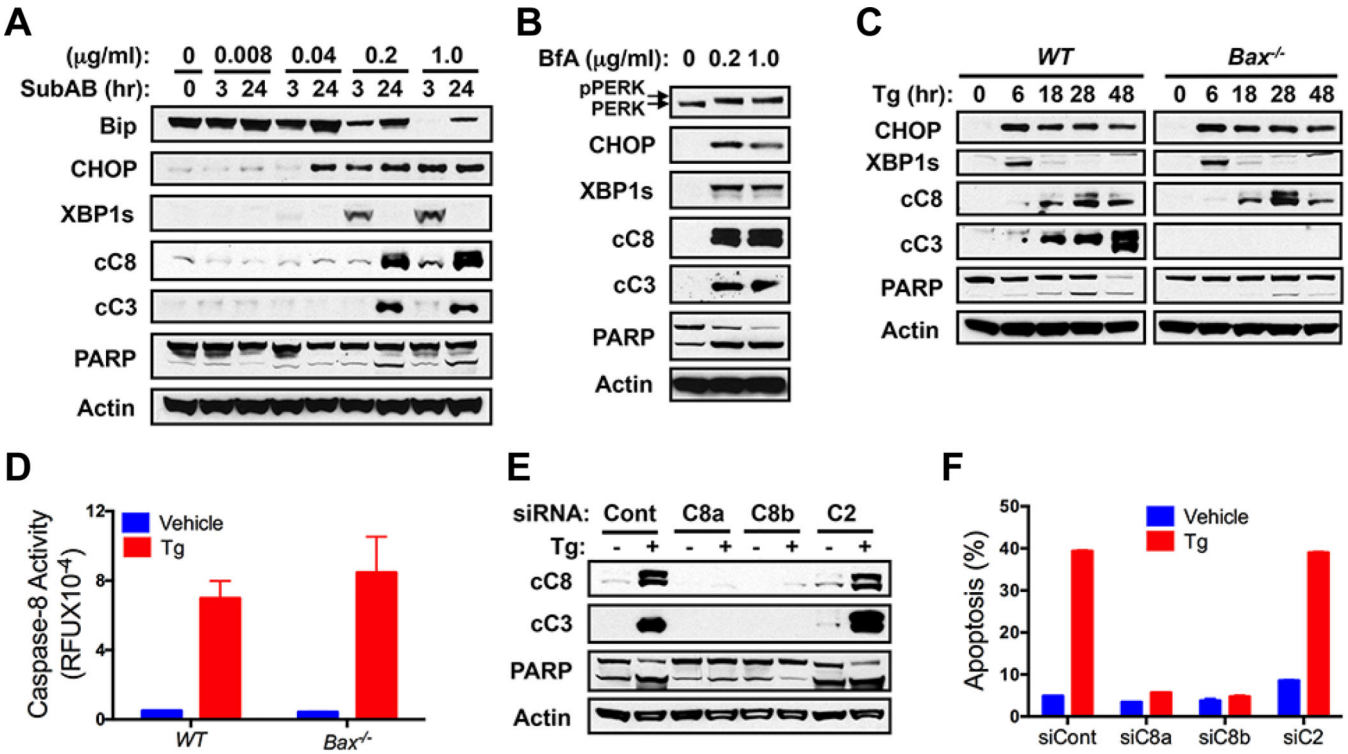

Fig. 1. Unmitigated ER stress triggers apoptosis via caspase-8

(**A**) KMS11 cells were treated with SubAB and analyzed by immunoblot. cC8: cleaved caspase-8; cC3: cleaved caspase-3. (**B**) SK-MES-1 cells were treated with BfA (24 hr) and analyzed by immunoblot. (**C** and **D**) Wildtype (WT) or *Bax*$^{-/-}$ HCT116 cells were treated with Tg (100 nM) and analyzed by immunoblot (**C**), or caspase-8 activity assay (24 hr) (**D**). (**E** and **F**) HCT116 cells were transfected (48 hr) with control siRNA, or a single (C8a), or an independent pool (C8b) of caspase-8 siRNAs, or caspase-2 siRNA. Cells were treated with Tg (100 nM) and analyzed by immunoblot (**E**) or FACS to measure apoptosis by subG1 DNA content (**F**). Graphs depict means ± SD of triplicates (**D**) or duplicates (**F**).

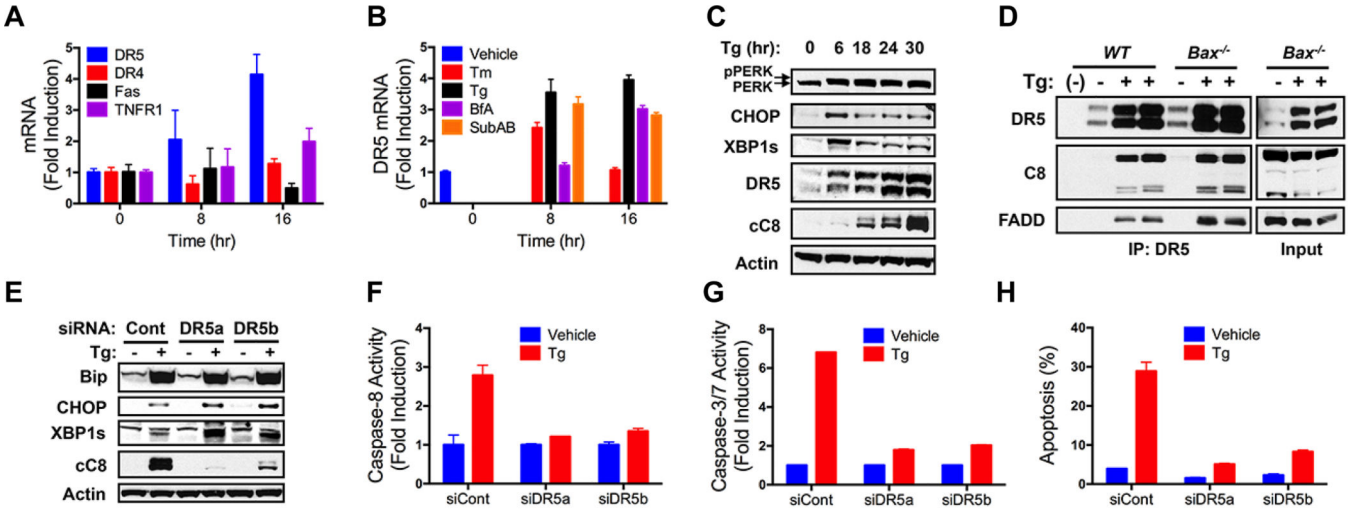

Fig. 2. Unmitigated ER stress activates caspase-8 via DR5

(**A**) HCT116 cells were treated with Tg (100 nM) and mRNA levels were measured by QPCR (normalized to GAPDH). (**B**) HCT116 cells were treated with Tm (1 μg/ml), Tg (100 nM), BfA (1 μg/ml), or SubAB (1 μg/ml) and analyzed by QPCR (normalized to GAPDH). (**C**) HCT116 cells were treated with Tg (100 nM) and analyzed by immunoblot. (**D**) WT *or* $Bax^{-/-}$ HCT116 cells were treated as in **C** (24 hr), subjected to DR5 IP, and analyzed by immunoblot. (**E–H**) HCT116 cells were treated as in **D** and analyzed for caspase-8 activity (**F**), caspase-3/7 activity (**G**) and apoptosis (**H**). Graphs depict means ± SD of triplicates.

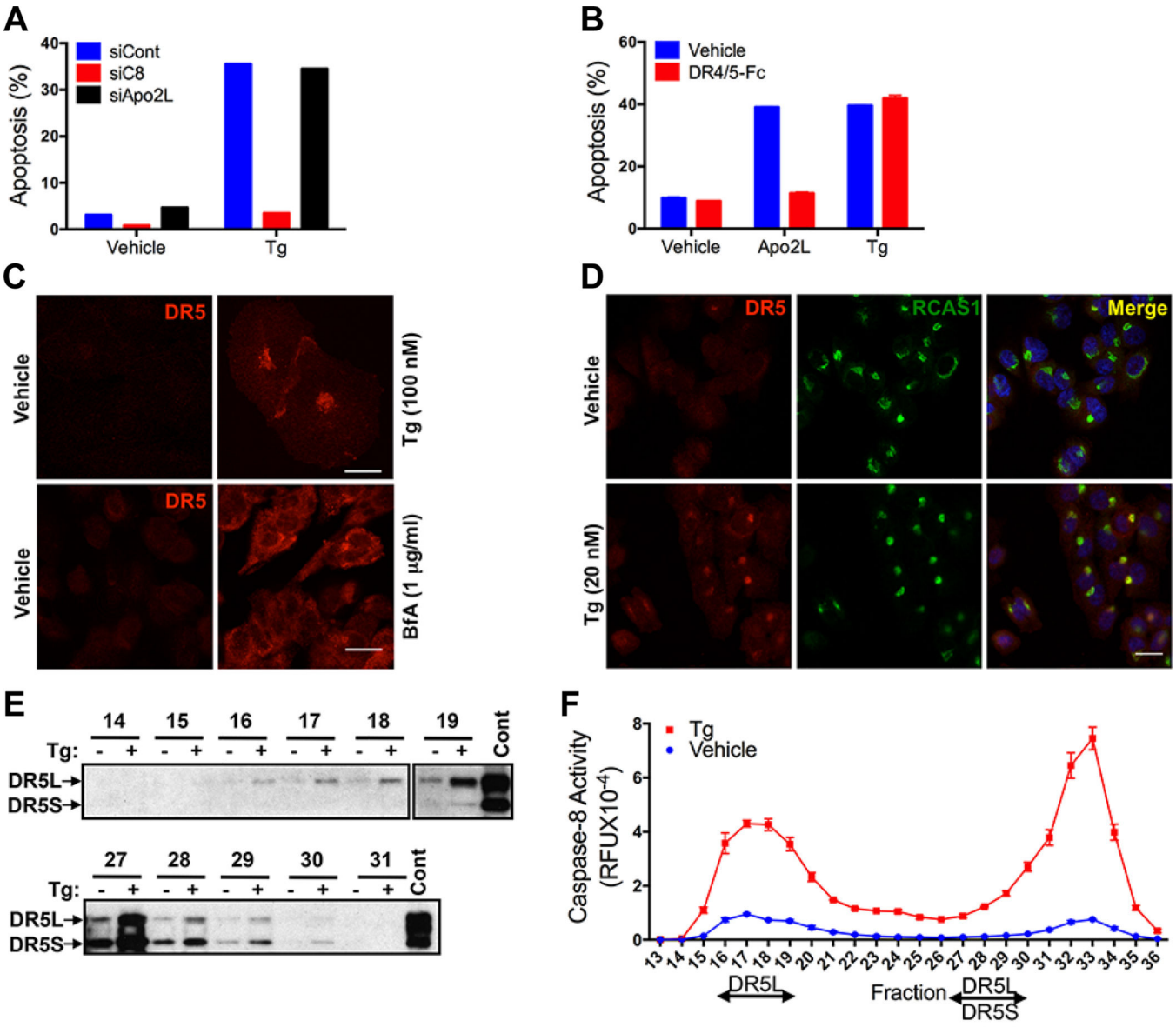

Fig. 3. Unmitigated ER stress engages caspase-8 by inducing ligand-independent intracellular DR5 activation

(**A**) HCT116 cells were transfected (48 hr) with control siRNA or siRNA targeting Apo2L/TRAIL or caspase-8. Cells were treated with Tg (100 nM, 24 hr) and analyzed for apoptosis. (**B**) HCT116 cells were treated (24 hr) with Apo2L/TRAIL (1 μg/ml) or Tg (100 nM) in presence of vehicle or DR4-Fc plus DR5-Fc (10 μg/ml each) and analyzed for apoptosis. (**C**) SK-MES-1 cells were treated (24 hr) with indicated ER stressors and analyzed by immunofluorescence with DR5-specific antibody. (**D**) SK-MES-1 cells were treated with Tg (20 nM, 24 hr) and analyzed by immunofluorescence for DR5 or RACS1. (**E** and **F**) HCT116 cells were treated with Tg (100 nM, 24 hr) extracted with 1% Triton X-100, and subjected to size exclusion chromatography; fractions were analyzed by DR5 IP and immunoblot (**E**) or caspase-8 activity assay (**F**): Control: direct DR5 IP from Tg-treated cells. Graphs depict means ± SD of duplicates (**B**) or triplicates (**F**).

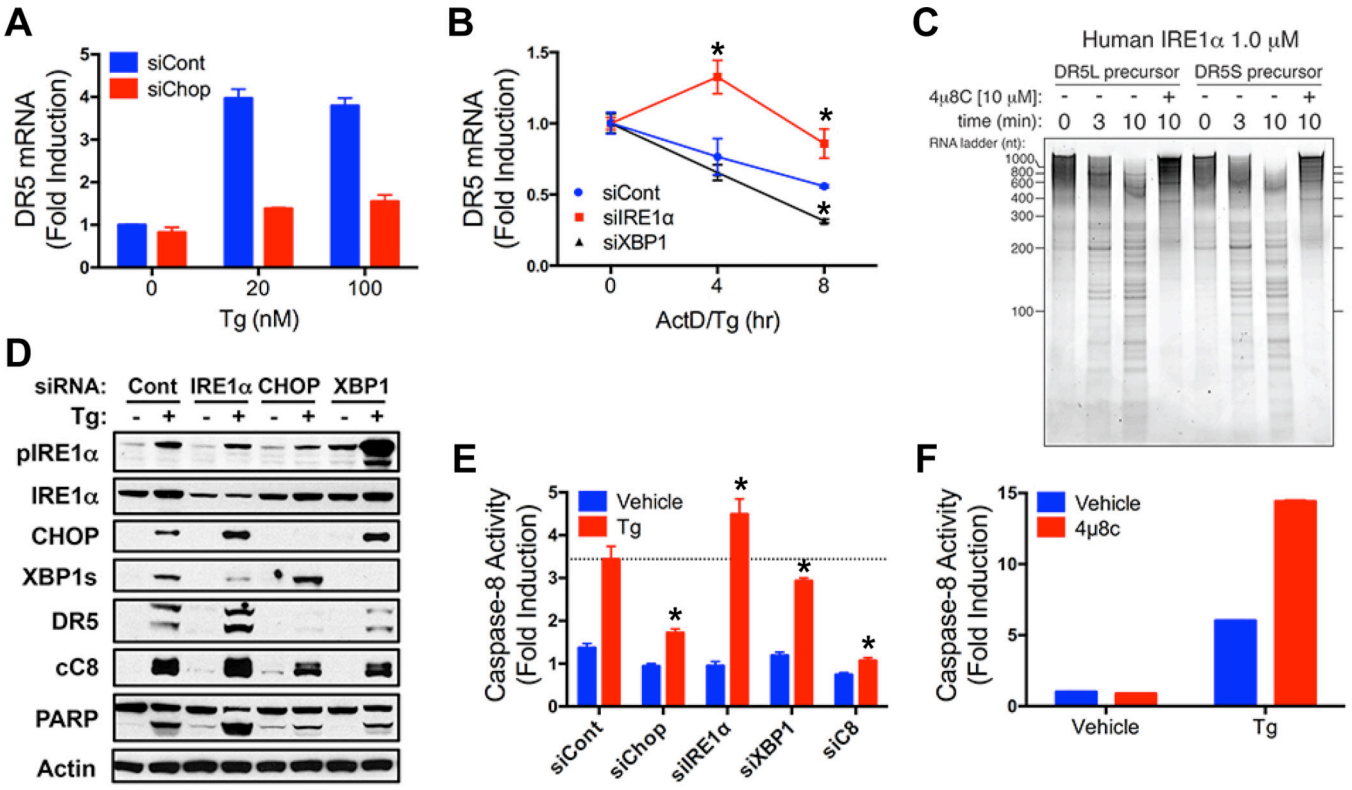

Fig. 4. DR5 integrates opposing UPR signals to control apoptosis

(**A**) HCT116 cells were transfected (48 hr) with control or CHOP siRNA, treated with Tg (8 hr), and analyzed by QPCR (normalized to GAPDH). (**B**) HCT116 cells were transfected (48 hr) with control, IRE1α or XBP1s siRNA, treated with actinomycin D (2 μg/ml) plus Tg (20 nM), and *DR5* mRNA was measured as in **A**. (**C**) Purified recombinant human IRE1α comprising the kinase and RNase domains (KR43) was incubated with in vitro-transcribed *DR5S* or *DR5L* mRNA in the presence of vehicle or 4μ8c (10 μM). Reactions were resolved on 6% TBE-Urea PAGE gels and stained with SYBR Gold. (**D and E**) HCT116 cells were transfected (48 hr) with control, IRE1α, CHOP, or XBP1s siRNA, treated with Tg (100 nM, 24 hr) and analyzed by immunoblot (**D**) or caspase-8 activity assay (**E**). (**F**) HCT116 cells were treated with Tg (100 nM, 24 hr) in presence of vehicle or 4μ8c (30 μM) and analyzed for caspase-8 activity. Graphs depict means ± SD of triplicates.